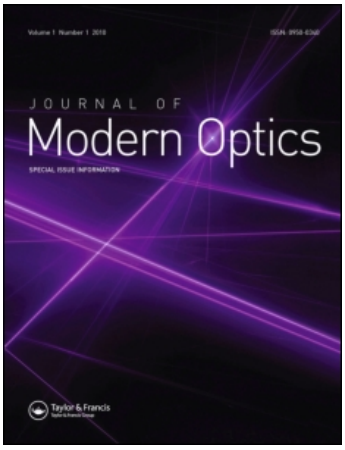

Journal of Modern Optics
Publication details, including instructions for authors and subscription information:
http://www.informaworld.com/smpp/title~content=t713191304

Supplementary active optics for illumination within an adaptive optics system

A. J. Lambert[a]; E. M. Daly[b]; E. deLestrange[b]; J. C. Dainty[b]
[a] School of Engineering and Information Technology, The University of New South Wales, Canberra, Australia [b] Applied Optics, School of Physics, National University of Ireland, Galway, Ireland

First published on: 13 April 2011

To cite this Article Lambert, A. J. , Daly, E. M. , deLestrange, E. and Dainty, J. C.(2011) 'Supplementary active optics for illumination within an adaptive optics system', Journal of Modern Optics,, First published on: 13 April 2011 (iFirst)
To link to this Article: DOI: 10.1080/09500340.2011.575239
URL: http://dx.doi.org/10.1080/09500340.2011.575239

Journal of Modern Optics
2011, 1–13, iFirst

Taylor & Francis
Taylor & Francis Group

Supplementary active optics for illumination within an adaptive optics system

A.J. Lambert[a]*, E.M. Daly[b], E. deLestrange[b] and J.C. Dainty[b]

[a]*School of Engineering and Information Technology, The University of New South Wales, Australian Defence Force Academy, Canberra, ACT 2600, Australia;* [b]*Applied Optics, School of Physics, National University of Ireland, Galway, Ireland*

(*Received 1 December 2010; final version received 17 March 2011*)

The use of additional adaptive optics to manipulate the beacon in an adaptive optics system for the human eye opens up many opportunities. Possibilities include better beacon creation, correction of gross aberrations that the beam acquires as it passes into the eye, symbiotic beams to guide or locate a probe or medical beam, and examination of the higher order aberrations experienced by the beam as it enters the eye. We describe the use of active optics for creation of the beacon in an adaptive optics system that incorporates a fundus imaging arm. In describing the possibilities for beacon shaping and steps that may be employed to use this to create a sharper or more versatile beacon, we determine the effects of such shaping on the performance of the system. Results are presented for both model and human eyes. The beacon shaping incorporates Bessel beam creation with tip-tilt and defocus correction from a mask on a spatial light modulator. Visual feedback from images of the beacon as it appears at the retina is used to refine it.

Keywords: adaptive optics; spatial light modulator; ophthalmology; Bessel beams

1. Introduction

An adaptive optics (AO) system relies on one or many beacons from which information is gathered about the aberrations the system is to correct. The aim of an associated imaging system is to gain near diffraction-limited images of the object of interest, such as celestial bodies in astronomy, the retina in ophthalmology, and the target in the case of surveillance. In astronomy, the beacon for wavefront sensing may be a natural guide star, or more likely a man-made laser guide star or beacon. In ophthalmology or vision science, the beacon is also man-made. The beacon delivery system forces light to enter the eye where it is focused to a reasonably confined point formed from the scattered light, and is hopefully relatively unperturbed by the aberrations experienced when traversing the eye's optics. In forming this beacon there is a trade-off between confinement of the spot, spatial attenuation and shaping of the light caused by the three-dimensional retina, and the scattered power received at the wavefront sensor (WFS). The traditional method in both astronomy and ophthalmology is to use a small diameter beacon to create a pencil beam that experiences less spatial aberration than an expanded beam, but that arrives at the scattering medium as a large spot. This of course gives a degree of averaging of the spatial characteristics of the scattering medium balanced by a reduction of power detectable by the WFS.

Should the beam forming the beacon on a retina also be the medical probe beam, any non-uniform scatter would negate the refinement that AO may bring, particularly in the extreme case where the scatter from the probe disappears as it interacts with the retina during surgery. So the alternative approach is to send the beacon through the AO correction system prior to entering the eye, such that the aberrations experienced are conjugated, and a tight diffraction-limited spot is formed provided the AO loop is successfully closed. It is worth noting that this method is not preferred in astronomy, or for flood-illuminated retinal imaging systems such as ours where scatter of the incoming light at various optical surfaces dominates over the weak return.

Regardless, the tight spot formed may be scattered in such a way that it is not detected by the WFS, nor in the imaging path should that be employed for guided surgery for example. Instruments such as the AO-supplemented scanning laser ophthalmoscope (SLO) [1–5] and optical coherence tomography (OCT) [5,6] devise an image of the retina by scanning a beam and integrating all scattered power at each location. Confocal techniques in SLO, and coherence gating in OCT, refine the depth and quality of the image but not the beacon guiding the AO. Variations in scattered power modulate these images, which – given that the retina is in motion during the scan – therefore require

*Corresponding author. Email: a.lambert@adfa.edu.au

ISSN 0950–0340 print/ISSN 1362–3044 online

DOI: 10.1080/09500340.2011.575239
http://www.informaworld.com

correction. This action is currently undertaken with software methods that register (with some latency) recent lines to relocate the received power to the true retinal location [2,4,7], or with tracking techniques implemented in hardware that alter the scan position [2,3,5]. A recent technique maintains a separated beacon for tracking retinal motion for refining the scan [5,6]. Such instruments would benefit from separate beacon creation, allowing for localised tip tilt applications to force the beacon to be formed at the desired location on the retina. They would also benefit from wavefront coding that provided a tighter spot (and hence higher axial resolution) upon correction of the aberrations experienced on beam entry to the eye, or for control/mitigation of the focus depth of the beacon. Currently, a tight beacon relies on the double-pass point spread function (PSF) where the same correction is applied to the beacon as to the imaging light due to the common correction path.

A surgical beam may be used to probe or operate on selected regions of the retina and may be supported by imaging through an AO system. In such an application, a co-located beacon and probe may allow detection of the site of interaction with the retina, without the need to observe the return from the probe beam. The beacon then acts as a target marker for the surgical beam. Such a shaped beacon would be equally applicable and provide benefits to many other applications of AO imaging systems.

Our suggestion is to place active optics in the beacon creation path of the instrument, and separate the AO system so as to shape the beacon for WFS to a more satisfactory result. We do this with a spatial light modulator (SLM) conjugate to the pupil of the eye. We assess the images of the beacon on the retina, obtained through the AO system at the science camera, in order to refine the active optics. At the moment, this refinement is by an operator observing the live images, but it could easily be machine controlled in a secondary AO control loop that is independent of, but encapsulates the primary instrument. The SLM can be illuminated by quasi-monochromatic light from a laser diode (LD) or super-luminescent light emitting diode (SLD). Unlike the achromatic deformable mirror typically used in an AO system, a liquid crystal display (LCD) can perform phase and\textbackslash or amplitude modulation of the illumination light. We give examples of special modulation masks that prove useful in refining the beacon. Note also that losses associated with such modulation, such as absorption and diffraction from the pixelated structure, are easily managed with increased source power while still satisfying maximum permissible exposure (MPE) restrictions.

Of course, the beacon shaping we have described requires an analysis of any effects it may impose on the primary AO system. Using a modified beacon, we demonstrate successful operation of an AO system based upon the pyramid WFS and incorporating a retinal imaging arm (reported in [8]). We present the temporal effects the beacon shaping has on the behaviour of the AO loop. Even though this paper is set in the context of ophthalmology, the findings are equally applicable elsewhere: to laser guide stars used in astronomy, to manufacturing using laser ablation where scattering in the working medium comes into play, and to multiple-object or multi-conjugate AO systems employed in surveillance imaging.

2. Separate active optics in the illumination

The traditional AO system, incorporating a science arm to image the retinal plane, is shown in Figure 1. The correcting element is controlled on the basis of the measurement of wavefront aberrations detected by a WFS. Whether the objective is wide-field imaging using a science camera, or single-point imaging as in the AO equipped SLO [1], it is necessary to arrange a beacon at the retinal plane with sufficient scatter to make a quality assessment of its corresponding wavefront emerging from the eye. Thus, if one is able to construct a beacon with improved scattering in the direction of the WFS, but still restricted by the limitations of the MPE, then the task of closing the loop and correcting the wavefront is expected to be more easily undertaken. For this purpose we include an active optic component in the beacon creation path shown in Figure 1. Here, a SLM is employed to spatially shape the beacon by manipulating the light using either phase or amplitude masks in a plane conjugate to the pupil of the eye.

The simplest modulation provides an additive tip and\or tilt to the wavefront so as to move the beacon around on the retina. A more complex modulation adds a defocus term to the phase to control the tightness of the beacon, for example in the presence of a subject's myopia. Still more complex and less obvious is to construct a beam with special properties such as a Bessel beam [9]. It is this beam and its combination with tip-tilt and focus components that this work concentrates on. However, there is no need to restrict the modulation to these terms alone, as a fully predicted wavefront correction may be modulated using this system to correct for the aberrations experienced by the beam on its path into the eye. This might be useful, for example, where the aberrations on the path into the eye are significantly different to those experienced by light exiting the eye.

The SLM we use as the active optic allows for modulation of pseudo-monochromatic light and it

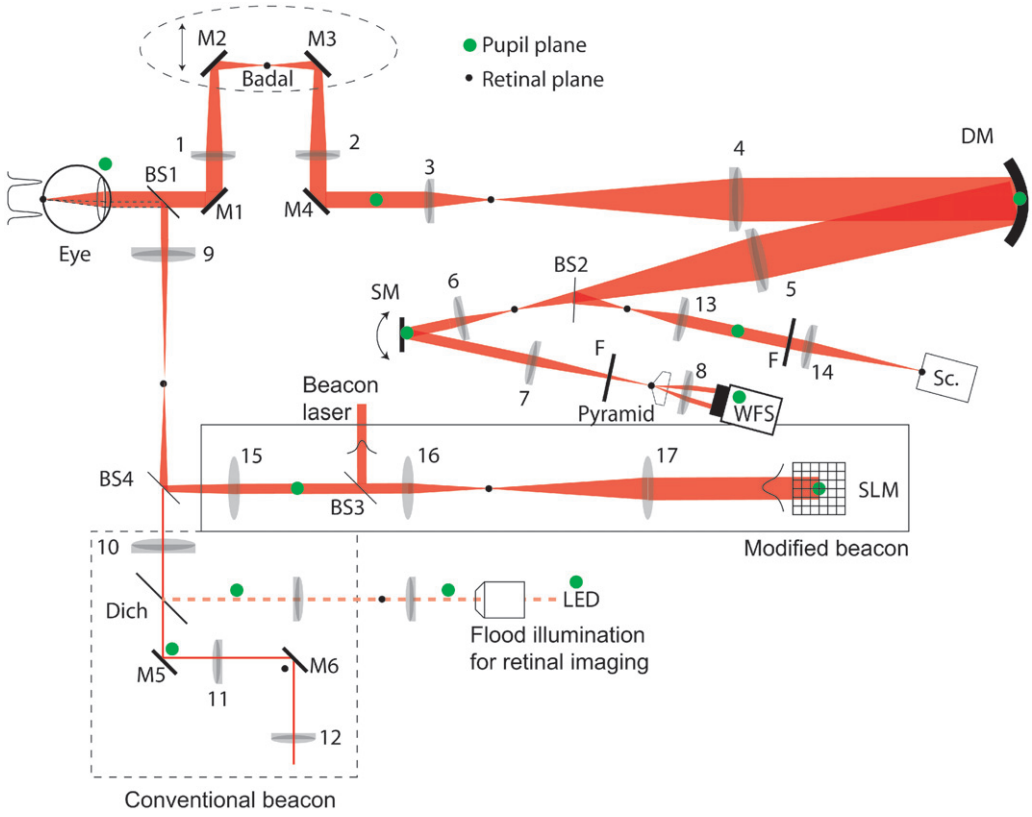

Figure 1. Schematic of the experimental AO system employing a pyramid wavefront sensor (WFS), deformable mirror (DM), and steering mirror (SM). The conventional beacon (pencil beam) is indicated by the dashed box, the modified beacon (shaped at the SLM) by the solid box. Images of the beacon are obtained at the science camera (Sc.) which is located at a conjugate retinal plane. The flood illumination arm for retinal imaging is shown entering the system at the dichroic (Dich); it is not used in the work presented here. Retinal planes are shown with small black dots, pupil planes with larger green circles. (The color version of this figure is included in the online version of the journal.)

does not need to be a continuous surface as phase wrapping is possible. Phase diversity of 2π is needed for the central wavelength for continuous grey-scale modulation, but only π if binary modulation is chosen. Binary modulation may be exploited to increase the diffraction efficiency, which is reduced when attempting grey-scale modulation at spatial frequencies that are attenuated by the modulation transfer function (MTF) of the SLM. This facilitates a reduction of the non-diffracted central spot that detracts from the desired beacon shape at the retina. In our experiment, the beacon is visible at the science camera. If different wavelengths were employed, a dichroic beam-splitter might form a useful path from which to observe the success of the active optics in forming the desired retinal construct, in the same way that this light is separated from the WFS.

The SLM can manufacture any desired (albeit pixelated), phase or amplitude mask, but we concentrate on simple beam shaping. Software controls the desired mask in the plane (x, y) that is conjugate to the pupil of the eye, to add the tip θ_{tip}, or tilt θ_{tilt}, about (x_{ot}, y_{ot});

$$H(x, y) = exp(j\theta_{tilt}(x - x_{ot})).exp(j\theta_{tip}(y - y_{ot})), \quad (1)$$

where $H(x, y)$ is a phase profile. A lens, zone plate, or 'chirp' in the paraxial approximation, of focal length f, is

$$H(x, y) = exp(j\alpha_x(x - x_{oa})^2).exp(j\alpha_y(y - y_{oa})^2). \quad (2)$$

When combined with the optics of the eye, the optical powers add giving defocus control over the axial location of best focus. Here $\alpha_{.} = \pi\Delta^2/\lambda f$, yields $\lambda\alpha_{.}/\pi\Delta^2$ dioptres of correction. Δ is the SLM pixel size projected onto the pupil, M is the number of pixels on the active region of the SLM, the effective diameter of the lens is $M\Delta$, and λ is the wavelength. Note that the off-axis chirp sited about (x_{oa}, y_{oa}) implicitly also includes a tip-tilt component [10].

The function that is used to form a Bessel beam is most interesting in this work;

$$H(x,y) = exp(j\sqrt{(\beta_x(x - x_{ob}))^2 + (\beta_y(y - y_{ob}))^2}), \quad (3)$$

where β is the Bessel coefficient. The annular shape of this beam around the focal plane of the eye optics is of interest in this application. Strictly this is not a true Bessel beam as we are only using the phase of the J_0 Bessel function associated with the Hankel transform of the annulus, but the effect is similar as it is predominantly the phase of the beam that determines the evolution of the spatial structure. The annulus has diameter $d = 2\beta\lambda f/\pi$ when Fourier transformed by a lens of focal length f, and β has units of m^{-1}. Interestingly, the shape of this annulus is maintained over a long axial length giving rise to its description as a cylinder, compared with the well known Gaussian beam waist.

The equations are written with separate origins on the SLM to show the degree of freedom that is offered. These centres in turn may not be concentric to the Gaussian beam that illuminates the device. Equation (2) exhibits astigmatism if the $\alpha_{\cdot}$ are different in x and y, and Equation (3) exhibits elliptic asymmetry if the $\beta_{\cdot}$ are different. The axes of each of these may be oriented differently.

One can imagine now a beam movable on the retina, with control over the focal plane position within the retina, that appears as a cylinder coming from an acute angle. Finally, these are all pure phase functions, and as such they can be multiplied together, and the real or imaginary component taken as an amplitude mask rather than a phase mask. In this case, the mask can be expressed as the desired phase object and its complex conjugate appears to travel in the reverse direction and hence seems to originate from behind the retina. For example,

$$H(x,y) = 2 + 2\Re e(exp(j\beta_r r)) = 2 + exp(j\beta_r r) + exp(-j\beta_r r) \quad (4)$$

where $r^2 = x^2 + y^2$. Note the undesired but necessary DC term that results in a central spot in addition to the two Bessel beams.

The binarisation of the above equations results in a superposition of spatial harmonics of the desired functions. This causes difficulties for tip and tilt with harmonic diffraction orders reproduced at odd multiples of the desired angle. In the case of the chirp it results in the creation of multiple focal planes at multiples of the desired axial position. In the case of the Bessel beam it creates sets of concentric circles or co-centred Bessel beams. In fact, any undesired non-linearities on the SLM will have similar effects, reducing the light in the desired place but adding terms that may be of benefit.

3. Commentary on the Bessel beam

While the inclusion of active optics within the beacon creation path provides the opportunity for any spatial phase or amplitude modulation, its use in the creation of a Bessel beam gives very interesting properties. The Bessel beam is described in the literature as 'non-diffracting', but in fact is better described as 'self-repairing' or as having a superior depth of field when compared with the Gaussian beam. Not only does the beam create a very interesting circular feature as its PSF in the image plane, but it holds this shape under Fresnel diffraction at planes spaced axially from the image plane. This leads to a description as a cylindrical waist, whereas a Gaussian beam has an 'hour-glass' waist. This is by virtue of the outer rings of its pupil mask rendering the annulus at different depths.

Interestingly, the Bessel beam has been described as self-repairing because light that converges to form its cylinder at longer axial distances does not travel the same path as light that may have been absorbed or scattered in the scattering media. Consequently, the light required to form the beam behind an obstruction finds its way around the obstruction and reforms that part of the cylinder, whereas the Gaussian beam is almost decimated by the obstruction. The net result is that the Bessel beam will penetrate to greater depths into the scattering medium such as the retina, but also will be spatially confined to the same radius annulus at subsequent distances into the media. This has been recently described from experimental observation [11], and is well known in laser machining where holes with straighter edges may be created to greater depths in material processing [12].

Once scattered (ideally back toward the WFS in our application), the light proceeds as if it were a Gaussian beam originating at the depth it was scattered from in the volume media; it will be destroyed by subsequent scattering and obstruction as it tries to exit the retina. The benefit of the Bessel beam thus only exists for the path entering the eye. Each point observed outside the eye on the annulus formed on or in the retina is rendered using the expected PSF of the optical system that is the eye. We are actively investigating this phenomenon and will report on this at a later date.

The long cylindrical waist of the Bessel beam brings another advantage. It is consequently robust to defocus errors, as would be experienced when examining a myopic human eye. Whereas a conventional beacon would result in a broadened and weakened

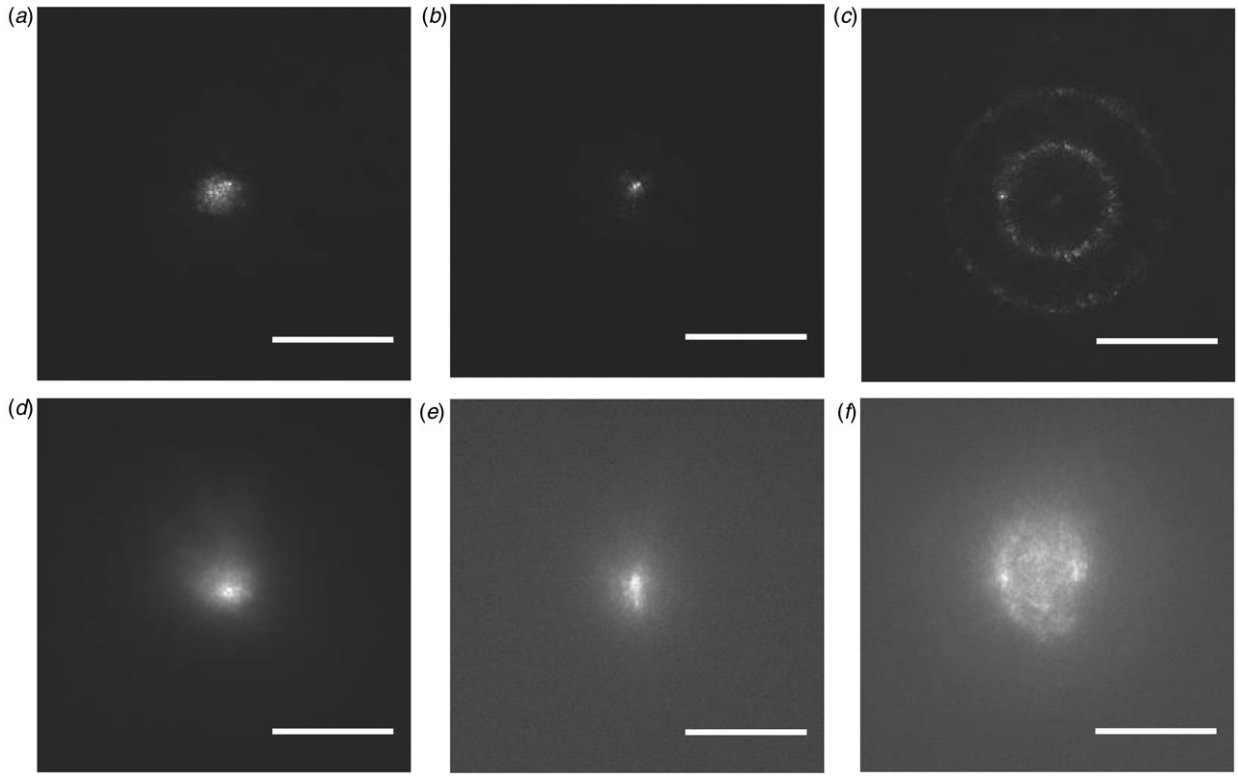

Figure 2. A beacon to be used for wavefront sensing in an AO system is projected onto the retina, and typical returns as seen at the science camera through the AO system are shown here. Top row: model eye (*a*) pencil beam illumination ($D < D_{pupil}$) – $P_{cornea} = 90$ nW; (*b*) large pupil illumination ($D \approx D_{pupil}$) - $P_{cornea} = 77$ nW; and (*c*) a Bessel illumination – $P_{cornea} = 77$ nW. Note the extra annulus caused by non-linearities in the SLM. Bottom row: human Subject A (*d*) pencil beam illumination - $P_{cornea} = 0.5$ μW; (*e*) large pupil illumination – $P_{cornea} = 0.2$ μW; and (*f*) a Bessel illumination – $P_{cornea} = 0.2$ μW. Images obtained with 10 ms exposure, sum of 20 frames. Scale bars correspond to 100 μm. In each case (model\real eye) the AO loop was closed on the conventional beacon and the deformable mirror was maintained at that static correction for all image acquisitions.

return from the retina as a result of defocus, especially for low f-number systems, the Bessel beam would produce an intact annulus reasonably immune to the defocus. The way this is counteracted in traditional low f-number (full pupil) systems is that the beacon passes through the AO correcting path on entry to the eye in order to form a compact spot when the AO loop is closed. See for example Figure 2(*b*). Of course this assumes there was enough return for the WFS to operate with the deteriorated state initially. Such is the case for pencil beam beacons where the light passes through only a small part of the pupil, resulting in a larger beacon, but one not deteriorated by aberrations in the path. See for example Figure 2(*a*). In both these traditional cases the power irradiating the cornea must be managed within MPE limitations and suitable signal-to-noise limitations of the WFS. In the case of the Bessel beam, the power budget must be similarly managed as the light is spread on the annulus (Figure 2(*c*)) rather than a tight point, but this is the case over a wide range of defocus. We show that this invariability of the radius of the annulus helps the closure of an AO system utilising this ring beacon. It is therefore much easier to observe the beacon from a human subject's eye that is less immobilised than would be required for a conventional beacon system. A subject with some accommodative response is more quiscent because the focus is not so critical. The subjects also report that it is easier and more comfortable to fixate on the ring\set of concentric rings than when observing the point beacon. A typical image seen by the subject is shown in Figure 3(*a*). This phenomenon of extended source viewing may also help relax the MPE limitations to allow for greater signal-to-noise at the wavefront sensor, or indeed exhibit a reduced hazard to the subject. The mechanism of energy dissipation in the retina will be different from the ring or cylinder than for the focused beacon on which the MPE intrabeam viewing restrictions are designed. (We do not enact such relaxed conditions because the SLM may fail to hold its mask pattern in our experiment, defaulting to a flat wavefront at the

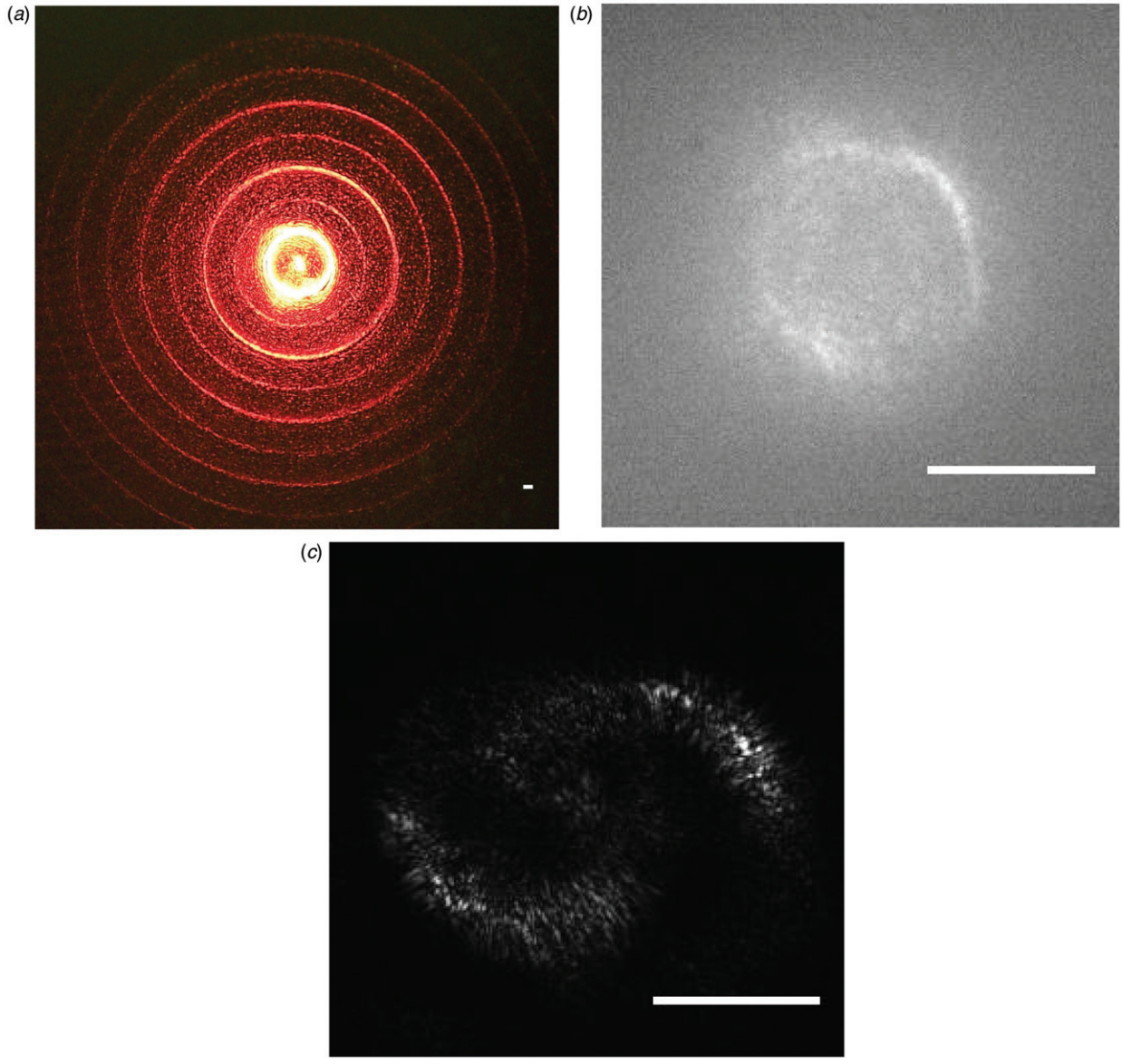

Figure 3. (*a*) A Bessel beam appears as an annulus whose width is set by the pupil diameter as with a normal beacon. Non-linearities in its generation result in other annuli concentric with the fundamental, but at multiples of the initial radius. Undiffracted light in the generation forms the usual shaped beacon at the centre. This is what a subject would see in visible light, but imaged here using a digital camera in place of the eye (F 4.5, 1s). (*b*) Vignetting of the illumination beam results in arcs dropping out of the annulus, as seen scattered from the retina of human subject B wearing their −1.5 D prescription – $P_{cornea} = 0.5\,\mu W$. (*c*) Introduction of tilt within the system separates the two Bessel beams that arise when using an amplitude mask in their generation. The result is two spaced annuli, hence carrying information about the aberrations experienced on entry to the eye. Here we show a vignetted, tilted beacon that might well be described as the 'essence of optics – or yin-yang' , from examination of an artificial eye – $P_{cornea} = 0.15\,\mu W$. Exposure for (*b*) and (*c*) was 10 ms. Scale bars correspond to 100 μm. (The color version of this figure is included in the online version of the journal.)

pupil and hence intrabeam viewing, but a suitable design interlock system would alleviate this concern. So the results presented here are for typical illumination power.)

The centre of the Bessel beam can be identified from the annulus seen for example in Figure 2(*c*) for a model eye, or even Figure 2(*f*) from a human subject, in spite of the loss of some of the circumference due to vignetting of the beacon. As mentioned, such a shaped beacon has advantages in its interaction with the scattering volume, such as the retina, that may benefit the likes of the SLO as well as direct imaging applications. It is an inevitable expectation that any change made to the beacon shape would affect the

evaluation of the wavefront and hence the performance of the AO loop. As the beacon shape looks more like an image of an extended source then different algorithms for processing it may need to be adopted. In the case of the circular grating or Bessel beam [9] a circle or set of concentric circles illuminates the retina, and it is this that is reproduced to the WFS. We expect that for the high f-number lenses used in the Shack–Hartmann (SH) WFS there will be little difference in performance as the annulus will not be resolved, but the pyramid WFS is more sensitive to extended source effects as it splits the image of the retina at the apex of the pyramid to balance the power in each quadrant.

4. Experimental system

The system schematic is shown in Figure 1. It is based upon the pyramid wavefront sensor with controllable tip-tilt modulation, a 19-channel OKO piezoelectric deformable mirror, and has been well reported previously [8]. The conventional beacon (dashed box in Figure 1) has diameter approximately 1 mm at the pupil, and it enters the eye 1.5 mm off-axis to avoid corneal reflections to the WFS camera. The modified beacon (solid box in Figure 1) operates at the same wavelength as the conventional one, 675 nm. It is collimated prior to entering the system at BS3, magnified using lenses 16 and 17, before illuminating a Hamamatsu PPMX8287 SLM that renders pupil conjugate masks in either amplitude or phase mode. This reflective-mode device is partially underfilled by the Gaussian source, and a 3.3× reduction in this field occurs on relaying to the pupil plane. The full width at half maximum (FWHM) of the Gaussian envelope that enters the eye is 3.5 mm, but the SLM projects onto a 6 mm pupil at the eye. A linear polariser inserted between lenses 16 and 17 is used to remove the majority of the undiffracted light, which returns from the SLM. This configuration is termed 'the phase-mostly mode of operation'. Images of our modified beacon, scattered from the retina, were collected using an Andor Luca EM247 Mono camera placed in a conjugate retinal plane (Sc. in Figure 1). The camera was cooled to −20°C, and typically 20 frames were acquired consecutively to allow for averaging of images. The camera pixel size is 10 μm.

Results were obtained from an artificial retina constructed by dissolving micrometre-sized glass beads in ink and painting them onto black paper. The magnification factor from this artificial retina to the science camera was ×9.4, so each camera pixel was equivalent to 1 μm at the artificial retina. For comparison, we show typical images obtained from the artificial retina when the beacon uses the traditional pencil beam in Figure 2(*a*), the full unmodulated SLM in Figure 2(*b*), and a Bessel modulated SLM in Figure 2(*c*). Notice the Bessel annulus has width similar to the PSF in Figure 2(*b*), and diameter set by the coefficient β.

Results were also obtained from the right eyes of two volunteers; subject A (30 years) is emmetropic and subject B (44 years) is myopic with a −1.5 D prescription. Subject A has a naturally low wavefront RMS error (0.116 μm) which is reduced to 0.044 μm on closing the AO loop on our system. Apart from the focus error, subject B also has a low error (0.123 μm with partial focus correction from the Badal stage fully at one end of its range) which is reduced to 0.063 μm on closing the loop. At the settings used to obtain these results, the wavefront reconstruction error in our system is 0.03 μm. Subjects were dilated using 0.5% Tropicamide, and stabilised using a bite bar aligned to the system. It is worth noting that measurements were possible when the subjects were not cyclopleged, having full accommodation and a reduced pupil. Example images from the retina of subject A are shown in Figure 2(*d*) for the original pencil beam beacon, in Figure 2(*e*) for an unmodulated SLM over the full pupil, and in Figure 2(*f*) with a Bessel modulation on the SLM. Occasional vignetting by the undilated pupil resulted in dropout of the full annulus from the beacon images, such as seen in Figure 3(*b*) for subject B. In an artistic twist, when amplitude modulation is employed on the SLM for a mask as described by Equation 4, and there is some vignetting accompanied by a tilt aberration, one observes a 'yin-yang' beacon. The two conjugate terms in Equation 4 are separated by the tilt that affects the beam on entry to the eye; the vignetting destroys part of each annulus, resulting in Figure 3(*c*), which one might call the 'essence' of optics. This work has received ethical approval from the National University of Ireland Galway Research Ethics Committee.

We operated below one tenth of the MPE (intrabeam viewing from IEC60825-1:2004 standard) of 69 μW at the illumination wavelength of 675 nm, using continuous viewing for periods of up to 30 minutes. The magnification factor for the real eyes was ×8.8 (assuming $f = 17$ mm), making each camera pixel equivalent to 1.1 μm at the retina. The fact that 768×768 pixels of the desired mask are optically rendered within the SLM to reduce pixelation effects comes with an accompanying reduction in MTF. This causes some non-linearities resulting in the extra rings seen in Figures 3(*a*) and 2(*c*). The analog bias voltage on the SLM is tuned to minimise the non-diffracted light. While there is a significant loss of power in this modulation scheme, it is not of concern for this work,

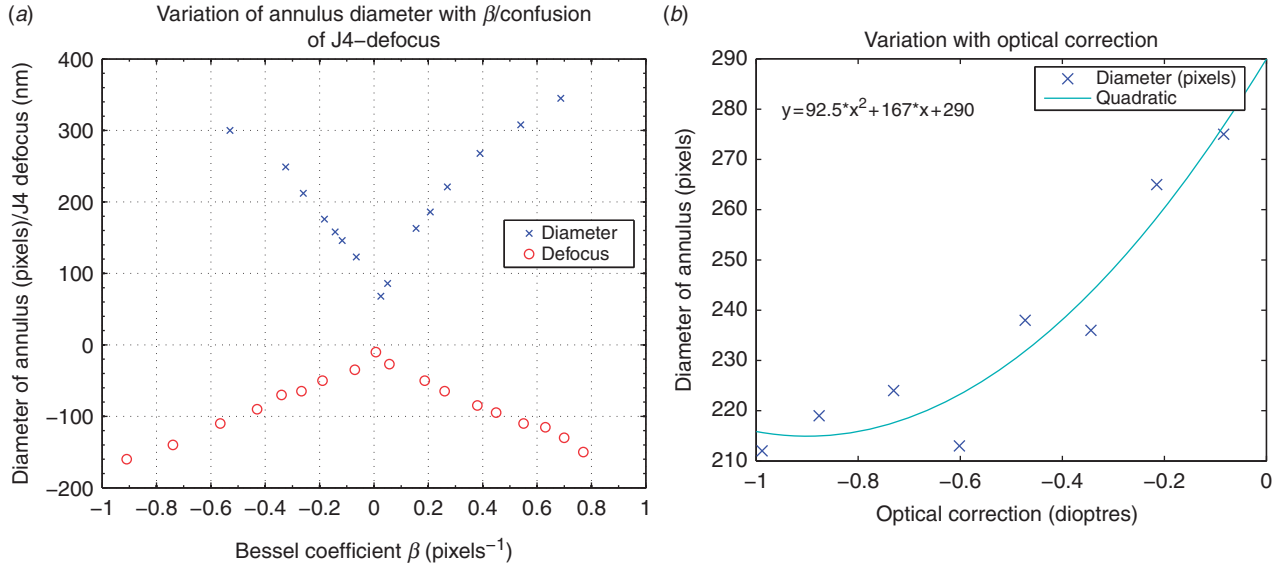

Figure 4. A Bessel beam may be generated using a phase or amplitude mask written on a pupil conjugated SLM. (*a*) The relationship between the radius of the resulting annulus on the retina of an artificial eye is shown against the coefficient, β_r on the SLM. The observed J4 defocus term as determined by the wavefront sensor is shown to be confused by the annulus also. (*b*) Also shown for $\beta = 0.249$ pixel^{-1} is the variation of this radius with added defocus, α_r, over the range of 1 dioptre from the initial correction of 1 dioptre. To obtain these results, the AO loop was closed using the conventional beacon and the DM maintained static at that correction. (The color version of this figure is included in the online version of the journal.)

as incident power can be increased to maintain power at the cornea at satisfactory but safe levels. For example, 0.41 mW at the output of the beacon laser results in 60 nW at the cornea. This is one advantage of keeping the beacon creation path separate from the imaging path to the science camera through the AO system; it would suffer scatter from optical surfaces at higher power levels, leading to a reduction in the achievable signal-to-noise ratio in the science imaging and wavefront sensing systems.

In terms of coefficients of Equations (2)–(3) a thin lens model of the eye renders an annulus of diameter

$$d = 2\lambda f \beta \Delta / \pi, \tag{5}$$

where β in units of pixels^{-1} is modified for pixel size, Δ, projected onto the pupil. The annulus width

$$w = 1.22\lambda f / D \tag{6}$$

is set by the lesser of that seen through the pupil of diameter D or the incoming beam diameter. In the case of the human eye, the focal length, f is variable between subjects. We tested the diameter against the desired β coefficient using a model eye. Results of this calibration are shown in Figure 4, and reinforce the relationship in Equation (5) for small β. Also shown in Figure 4(*b*) is the effect of adding defocus to the SLM mask as this changes the annulus diameter (shown for $\beta = 0.249$ pixel^{-1}). The sharpest image of the Bessel annulus was formed using a chirp contribution on the SLM. This is approximately one full dioptre of correction. Then the chirp coefficient was altered over another full dioptre, and the resulting beam diameter determined from the beacon images. There is little variation in this diameter over the defocus range. Any variation in focus effectively turns the cylinder beam into a conical shape, but the annulus thickness tends to stay the same over a range of a few dioptres of defocus, making it very useful in obtaining a beacon return for subjects requiring moderate optical correction where a Gaussian beam would be too spread, requiring a Badal or trial correction lenses and human intervention to correct the subject's prescription. To illustrate the performance in a human eye we show in Figure 5 the radially averaged cross-section of the Bessel annulus formed on the retina of the right eye of subject A and imaged through the science arm of our system. We also include for comparison the same for a conventional beacon. All results were obtained in closed-loop with the DM static at the correction calculated using the conventional beacon. As this subject is emmetropic, the Badal stage was not used. The radial cross-sections shown have been identified about the centroid of a background eliminated average (non-registered) of 20 frames for each curve. The cross-sections are normalised for the occurrence of values from the discrete image grid at that radius, and further normalised for exposure time and power supplied to

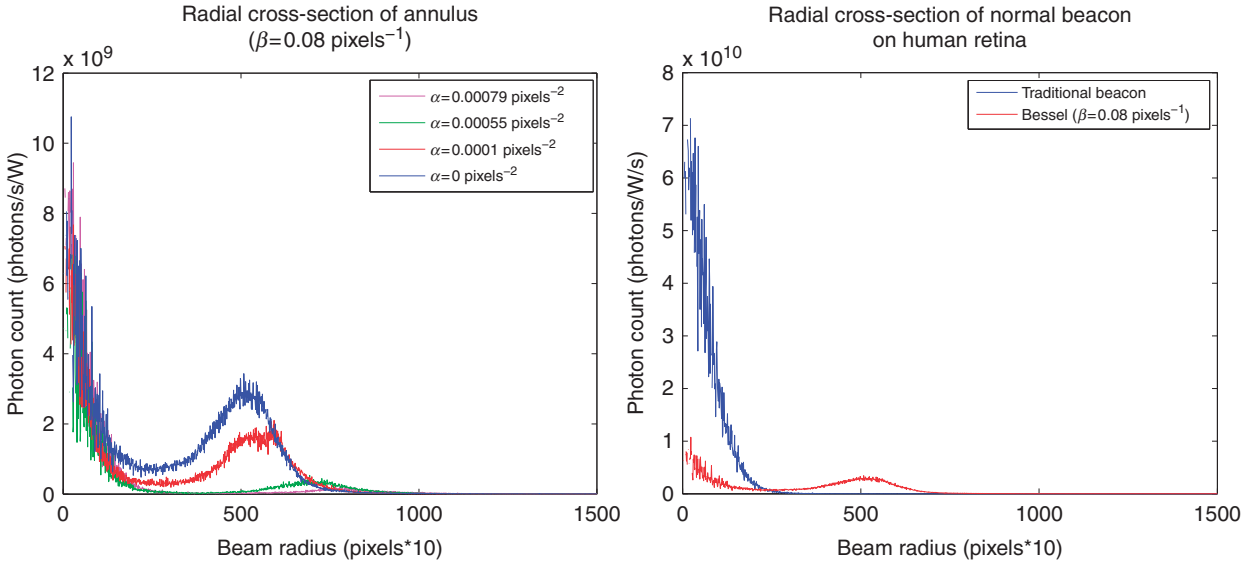

Figure 5. (*a*) Radially averaged cross-sections of in-focus and defocused Bessel annuli ($\beta = 0.08$ pixel^{-1}); defocus amount is 0.02, 1.18, and 1.69 dioptres, corresponding to $\alpha_z = 0.0001$, 0.00055, and 0.00079 pixel^{-2}, respectively. (*b*) For comparison the result obtained using a full-pupil beacon from a flat SLM is also shown. For scale, the red curve in part (*b*) is the same as the $\alpha_z = 0$ curve from part (*a*), so no defocus has been added to the beam. A Bessel beam exhibits a much longer waist axially than a Gaussian or diffraction-limited beam. When interacting with a volume scatterer such as the retina this is important to ensure maximum scattered and localised light for wavefront sensing, but also has the advantage that the beacon creation is much less sensitive to defocus. (The color version of this figure is included in the online version of the journal.)

the cornea. Hence, the vertical axis is in the units: detected photons/s/W. The centroid has been confirmed as reasonable by visual investigation of the images, and lends weight to the notion that the annulus may be a good locator for an accompanying surgical beam. Surface fitting of the annulus in Matlab also concurs with these observations.

5. Estimation of wavefront aberrations resulting from a shaped beacon

If beacon shaping is to be exploited in the dynamics of the AO system, its effect must be quantified. If the goal is to aid the performance of loop closure, the beacon must interact with the system dynamics; if the beacon is to be an aid to the medical operation or diagnostic imaging, it should not impinge on the system dynamics. To this end we examine the particular use of a Bessel beam and its accompanying annulus on the retina. As the radius of the annulus is a function of the spatial frequency of the mask on the SLM, we need to examine the effect that changes in this radius have on the initial estimation of wavefront aberration using the beacon, and the ability of the system to perfect the wavefront correction using this beacon.

The pyramid sensor splits the image field, and hence the annulus, at its apex into four quadrants and analyses the power balance in each. It is reasonable to expect that the annulus might balance just as well as the conventional beacon PSF if it is contained in the field of view of the sensor and centred on the apex. However, if it is off-centre, and depending on its radius, it might have a changeable effect, and might be described as a defocused point source in some scenarios. Of course, changing the defocus with the wavefront corrector would soon identify little change in the annulus, and hence add the possibility of rejection of this erroneous estimation, in much the same way as a badly defocused traditional beacon might interact with the loop. Vignetting effects such, as shown in Figure 3(*b*), will change the balance, as would any asymmetry in the traditional beacon scatter. The pyramid WFS should reject this. In saying this we should still note that the field of view subtended by the annulus is most likely well within an isoplanatic angle.

The other contributing factor is the possibility of the annulus subtending more than the field of view of the sensor, and wavefront estimation operating from no signal. For reasons similar to this, the pyramid sensor is accompanied by a tip-tilt mirror that dithers the field over the apex of the pyramid. This range of tip-tilt or modulation extends the field of view over which the pyramid can cope with retinal or beacon movement, and also serves to reduce speckle effects through time-averaged exposures. It is expected that

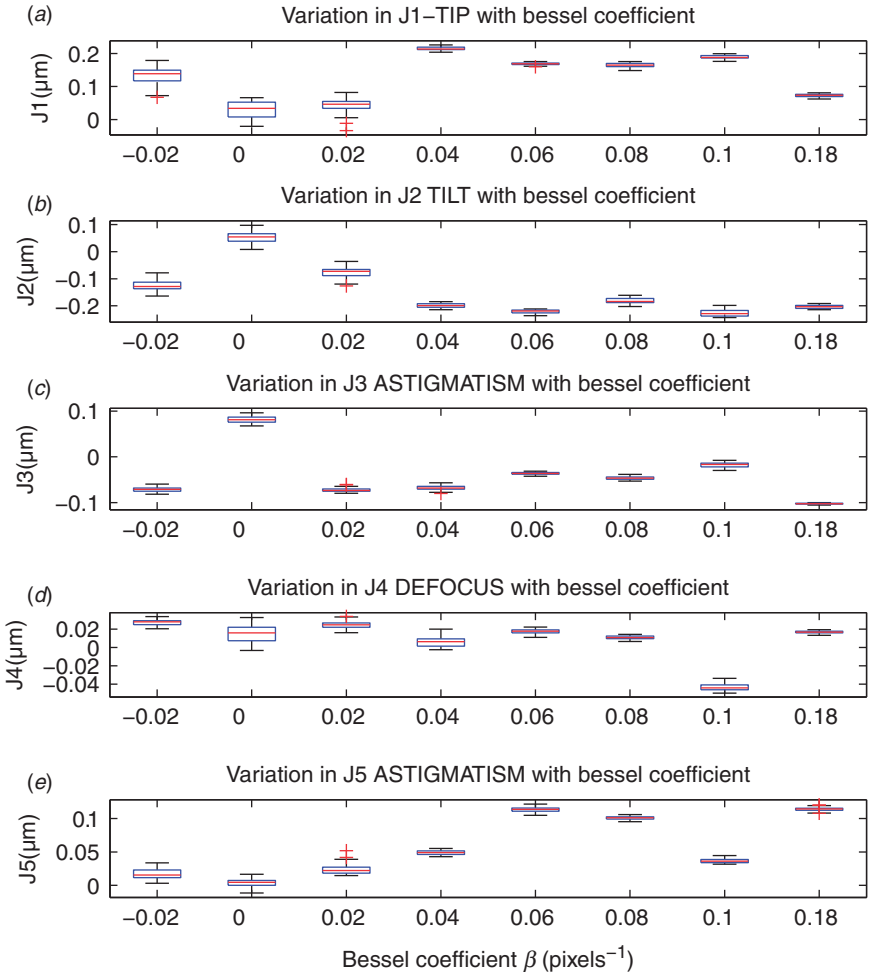

Figure 6. A Bessel beam creates an annulus as the beacon seen by the WFS. This is shown to result in an erroneous estimation of defocus by the WFS in open loop observation. Other aberrations exhibit similar errors. Expressed here as Zernike coefficients (*a*) J1 – tip; (*b*) J2 – tilt; (*c*) J3 – astigmatism; (*d*) J4 – defocus; (*e*) J5 – astigmatism; we see the relationship of this error with Bessel coefficient. (A wider annulus results from a larger Bessel coefficient.) In the error bars the central mark is the median, the edges of the box are the 25th and 75th percentiles, the whiskers extend to the most extreme datapoints the algorithm considers to be not outliers, and the outliers are plotted individually. These results were obtained from an artificial eye. (The color version of this figure is included in the online version of the journal.)

there will be a coupling in the estimation and loop closure performance of this modulation with the Bessel coefficient that governs the radius of the annulus.

To test these phenomena, we used a model eye illuminated by a programmable Bessel beam, and examined the effect on the wavefront estimation in open loop, and the rate of loop closure from this open loop estimate to equilibrium closed loop error. For comparison, we undertook the same with the conventional beacon, and the full-pupil illumination with the flat SLM (hence creating a diffraction-limited beacon). The wavefront estimation and expansion into Zernike coefficients, and the reduction in these coefficients and the total wavefront RMS over time from loop closure were acquired using the software described in [8].

5.1. Open loop estimation of aberration in the presence of a Bessel beam

Figure 6 shows the effect of the Bessel coefficient β_r on the estimation of each term of the wavefront expansion into Zernike polynomials. The combined effects of these and other higher order aberrations comprise the similar result for total RMS wavefront error seen in Figure 4. The OSA standard [13] labelling for the coefficients is used, and determination is over a 6 mm pupil. For larger Bessel coefficients, β, the annulus is wider. Of note is that there is coupling of the wavefront expansion terms to this increased radius of the annulus, but when the annulus is too wide so as not to appear in the pyramid sensor field of view,

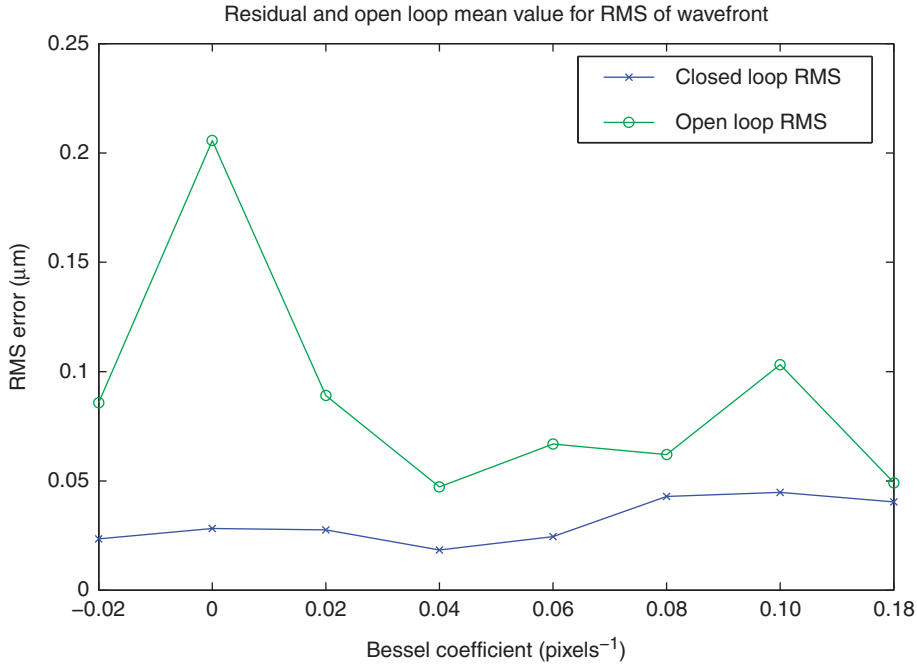

Figure 7. RMS wavefront error obtained from an artificial eye using a shaped Bessel beacon on the pyramid WFS based AO system. Open and closed loop operation is shown. The RMS wavefront error (tip-tilt removed) is found to be a function of the annuli radius, but the AO system is able to close to a very good Strehl (low RMS) regardless. (The color version of this figure is included in the online version of the journal.)

the estimation does not appear to be perturbed to the same extent.

5.2. *Closure of the AO loop in the presence of Bessel beam*

A figure of merit of an AO system is how much reduction in RMS error in the wavefront occurs when the loop uses the beacon to close to an appropriate correction. Figure 7 shows that the RMS wavefront error being corrected by the mirror is reduced after the loop is closed, for all Bessel coefficients. At first glance the open loop RMS error appears less when the Bessel beam is employed, with the largest value for open loop RMS occurring when the SLM was flat – the beacon then is a diffraction-limited spot rather than a Bessel. However, the lower estimations when the Bessel annulus is used as the beacon may just be due to averaging of the individual Zernike terms, confused by the Bessel beam as shown in Figure 6. Nevertheless, the RMS is reduced to similar levels when the loop dynamically closes. In all cases the loop was able to close to an RMS residual error of less than 0.04 µm, corresponding to a Strehl of ≈0.6 at the system wavelength of 675 nm. This improvement is modest but as expected for the limited correction possible with the OKO mirror, and commensurate with results obtained when operating with a conventional beacon. In all cases, observation of the retinal image of the beacon confirmed it was obtaining the sharpest image of the annulus and not being confused by defocus seen in open loop measurement. This simple result suggests that the AO system will perform in the presence of the Bessel-shaped beacon.

5.3. *Effect on dynamics of the AO loop*

A simple model for the dynamic system was proposed in [8]. Matlab's curve-fitting toolbox and System Identification toolboxes were employed to find a first-order fit to the step responses representing the reduction in RMS wavefront error when transitioning from open loop operation to closed\correction of the aberrations. Six seconds of wavefront estimation data is used, with approximately the first 2 seconds containing the open loop values. It is not hard to locate the position of the loop closure in these sequences. The steady state is set to the mean of the RMS error of the latter samples, and a step fall time is then determined for each sequence. It should be noted there is evidence of third-order system performance with the bounce in the step response found in some sequences. We have ignored this in estimating the fit as it did not occur in all traces. Figure 8 demonstrates the

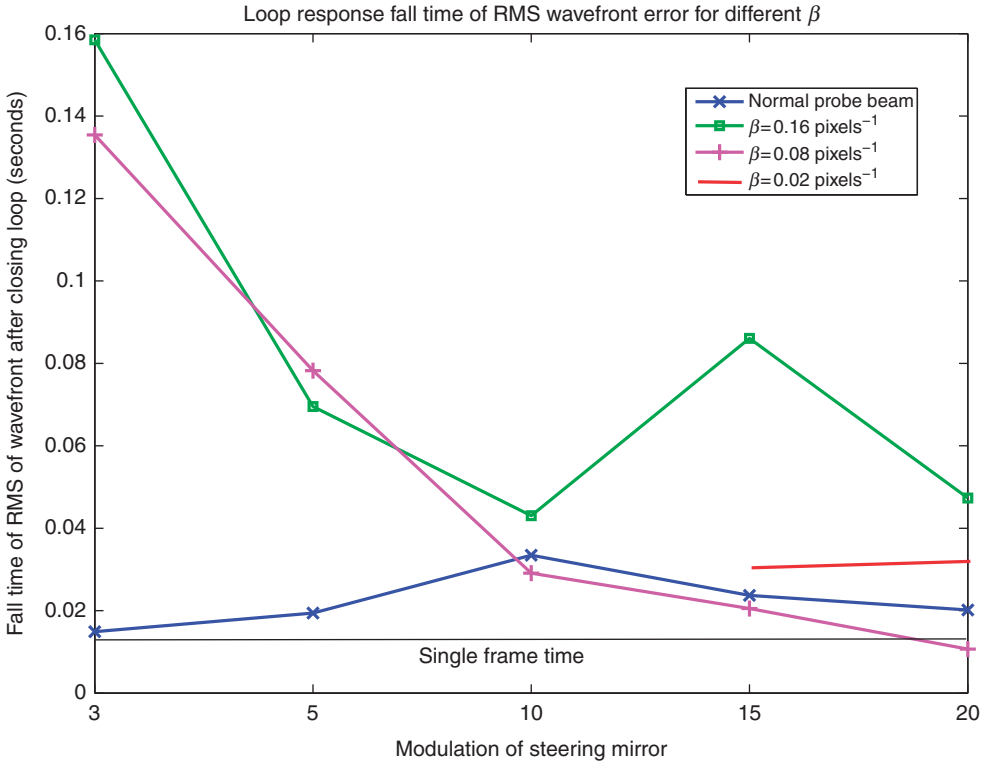

Figure 8. While the AO loop will close in the presence of a Bessel beacon (see Figure 7), there is a small penalty in terms of response time. The loop closure time expressed as evolving RMS error (increasing Strehl) is examined as a step response of a single pole system and exhibits fall times linked to the radius of the annuli. Using an artificial eye the fall time is plotted against Bessel coefficient, and compared with the performance with a conventional beacon. In the pyramid sensor, loop gain can be altered by adjusting the modulation of a tip-tilt mirror (SM in Figure 1) placed before the pyramid. The amount of tip-tilt modulation is shown on the horizontal axis to show its contribution to loop closure. (The color version of this figure is included in the online version of the journal.)

fall time found for each sequence where the Bessel coefficient and the pyramid WFS modulation range is changed for each. The trend of reduced response time at larger modulation is shown regardless of the Bessel coefficient, as is the trend that for a given modulation the convergence is slower for the larger annulus radius. For comparison, we show operation with the conventional beacon, and the horizontal line indicates 1/frame rate of the camera which is the fastest our loop is updated. Where curves fall below this limit is just an indication of the error in estimating the step response time. The control loop gain described in [8] was set at 0.5, and the wavefront sensor was binned to 4×4 pixels to balance spatial sampling with increased frame rate for all observations.

6. Conclusion

The use of active optics within the beacon creation path of an AO system to aid the creation of a beacon for wavefront sensing has been outlined. While it can conceivably provide any spatial modulation to correct intervening aberrations, or create a shaped beacon or constellation of such, its power is shown for much simpler masks. For example, the addition of tip-tilt, defocus using a chirp, and, in particular, the functionality afforded by a Bessel beam, are invaluable experimental tools. Feedback through the imaging path describing the successful shaping on the beacon will allow for a secondary adaptive optics path, independent of the AO operation. We have also investigated the performance of a traditional AO system in the presence of this beacon shaping. We have shown that, while it does couple to the working of the AO, it still allows successful operation of that system, albeit with slightly slower dynamic correction at the instant the loop is closed. This should not further affect the operation or speed of the closed loop. We see one of the major applications of this beacon shaping for when it is accompanying a surgical or probe beam to provide precise targeting, where the central beam might not be observable because of its interaction with the retina.

Acknowledgements

The first author would like to thank NUI Galway for supporting some of this work while he was there on sabbatical. This work was supported in part by SFI Grant SFI/07/IN.1/1906.

References

[1] Roorda, A.; Romero-Borja, F.; Donnelly III, W.J.; Queener, H.; Herbert, T.J.; Campbell, M.C.W. *Opt. Express* **2002,** *10,* 405–412.

[2] Yang, Q.; Arathorn, D.; Tiruveedhula, P.; Vogel, C.; Roorda, A. *Opt. Express* **2010,** *18,* 17841–17858.

[3] Ferguson, R.; Zhong, Z.; Hammer, D.; Mujat, M.; Patel, A.; Deng, C.; Zou, W.; Burns, S. *J. Opt. Soc. Am. A* **2010,** *27,* A265–A277.

[4] Li, H.; Lu, J.; Shi, G.; Zhang, Y. *Biomed. Opt. Express* **2010,** *1,* 31–40.

[5] Mujat, M.; Ferguson, R.D.; Patella, A.H.; Iftimia, N.; Lue, N.; Hammer, D.X. *Opt. Express* **2010,** *18,* 11607–11621.

[6] Zawadzki, R.; Jones, S.; Olivier, S.; Zhao, M.; Bower, B.; Izatt, J.; Choi, S.; Laut, S.; Werner, J. *Opt. Express* **2005,** *13,* 8532–8546.

[7] Vogel, C.; Arathorn, D.; Roorda, A.; Parker, A. *Opt. Express* **2006,** *14,* 487–497.

[8] Daly, E.M.; Dainty, C. *Appl. Opt.* **2010,** *49,* G67–G77.

[9] Dyson, J. *Proc. R. Soc. London, Ser. A* **1958,** *248,* 93–106.

[10] Davis, J.; Guertin, J.; Cottrell, D. *Appl. Opt.* **1993,** *32,* 6368.

[11] Fahrbach, F.O.; Simon, P.; Rohrbach, A. *Nat. Photonics* **2010,** *4,* 780–785.

[12] Matsuoka, Y.; Kizuka, Y.; Inoue, T. *Appl. Phys. A* **2006,** *84,* 423–430.

[13] Thibos, L.N.; Applegate, R.A.; Schwiegerling, J.T.; Webb, R. *Vision Science and its Applications*, Vol. 35, Trends in Optics and Photonics Series: V. Lakshminarayanan, Ed.; Optical Society of America, 2000; pp 233–244.